Stessa 2009 – Mazzolani, Ricles & Sause (eds)
© 2009 Taylor & Francis Group, London, ISBN 978-0-415-56326-0

Experimental seismic testing of a controlled rocking bridge steel truss pier

M. Pollino
Simpson, Gumpertz, & Heger Inc., Waltham, MA, U.S.A

M. Bruneau
University at Buffalo, Buffalo, NY, U.S.A

ABSTRACT: The experimental seismic testing of a 1/5-length scale model, slender bridge steel truss pier was conducted to investigate the use of a controlled rocking approach as a means of seismic protection. The controlled rocking approach allows the pier to uplift from its base, partially isolating the structure, while passive energy dissipation devices (steel yielding devices, fluid viscous dampers) are implemented across the uplifting location to control the response. The controlled rocking approach for seismic protection limits the force demands placed on the bridge pier and deck and can allow the structure to remain elastic during an earthquake, preventing damage, and increasing the probability that the bridge remains operational following the earthquake. The experimental specimen's design, set-up, and selected testing results are presented. The testing program included the use of three sets of steel yielding devices and a set of fluid viscous dampers while the model was subjected to ground motion records using three components of motion. Experimental results are presented and compared with the expected fundamental behaviour (self-centering, hysteretic behaviour, higher mode participation) which is evident in the experimental results. Comparisons between the experimental results with design predictions and advanced analytical methods (nonlinear time history analysis) are made that show reasonable prediction of response.

1 INTRODUCTION

As the focus on the seismic design of critical structures shifts from a methodology that aims to achieve collapse prevention and life-safety (allowing damage to structural members) to one that focuses on limiting downtime (or keeping structures fully functional) following major seismic events, approaches for the seismic retrofit of existing bridges or design of new bridges that provide this increased level of performance, at a reasonable cost, are needed.

More recently, the reliance on stable rocking to provide satisfactory seismic performance has received a renewed interest: more research is being conducted on this topic and various levels of rocking response have been considered in the retrofit of large bridges. This is in part due to a growing appreciation for the ability of such systems to efficiently withstand seismic demands elastically with little to no damage while providing a self-centering ability. Thus rocking behavior, if properly designed, can meet important seismic performance objectives such as elastic response of the structure while re-centering following an earthquake.

As part of this ongoing research, Pollino and Bruneau (2007) have investigated the fundamental behavior of the controlled rocking approach of 2-legged piers that uses steel yielding devices at the base of bridge piers and developed a design approach that can be used to calibrate the devices to control response and meet design objectives. Additionally, the dynamic behavior of controlled rocking bridge steel truss piers is discussed in Pollino and Bruneau (2008a) that addresses the participation of higher modes in the controlled rocking response resulting from the impacting and uplifting of pier legs with their foundation.

This paper discusses the seismic testing of a 1/5-length scale model, slender bridge steel truss pier that uses the controlled rocking approach for seismic protection of a bridge. The experimental specimen's design, set-up, and selected testing results are presented. Peak response results are compared with design predictions (developed through fundamental understanding of system behavior) and with nonlinear time history analysis.

2 PROTOTYPE PIER

Prototype pier properties are based on a brief review of drawings of existing bridges supported on steel truss piers. The prototype bridge pier is assumed to support a segment of a 2-lane highway bridge deck between the bridge's abutments. The pier is assumed

to have a tributary inertial mass in the longitudinal and transverse directions equal to its vertical mass. Prototype pier properties deemed relevant for dynamic testing are given in Table 1. Photographs of two-legged and four-legged bridge piers of this type are shown in Figure 1. Incidentally, these piers have been retrofitted by allowing them to rock (Dowdell and Hamersley, 2001), although the specimens are not meant to be exact model replicas of those specific two piers.

3 EXPERIMENTAL MODEL

3.1 *Similitude scaling*

The artificial mass simulation scaling law that has been used in many experimental tests investigating response of structures to earthquakes (Harris and Sabnis, 1999) has also been followed here. For constant acceleration scaling and since the model is made of the same material as the prototype (steel), the acceleration scale factor, λ_a, and the elastic modulus scale factor, λ_E, are equal to one. Using this scaling law, the required model properties and properties provided after modifications required for controlled rocking design are shown in Table 1. A photograph of the specimen on the 6DOF shake table is shown in Figure 2.

Table 1. Prototype and model pier properties.

		Model	
Quantity	Prototype	Req.[a]	Prov.[b]
Pier height, h (m)	29.3	5.86	6.09
Pier width, d (m)	7.32	1.46	1.52
Pier aspect ratio, h/d	4.0	4.0	4.0
Inertial mass (kN/g)	1730	69.2	80.1
Gravitational weight (kN)	1730	69.2	80.1
Material modulus (GPa)	200	200	200
Pier lateral stiffness (kN/mm)	12.6	2.52	3.00
Lateral period of vibration (sec)	0.74	0.33	0.33
Vertical period of vibration (sec)	0.13	0.058	0.040
Vertical "Shearing" period of vibration (sec)	0.12	0.054	0.062

[a] Required model properties for similitude requirements.
[b] Theoretical model properties provided by the specimen.

(a) (b)

Figure 1. Typical prototype steel truss bridge piers (Courtesy of Bruce Hamersley, Klohn Crippen Berger Ltd.) (a) two legged piers and (b) four legged piers.

3.2 *Specimen design and boundary conditions*

The experimental specimen (originally designed for different testing programs) was modified to satisfy similitude and strength requirements, to allow rocking at the base, and to provide adequate boundary conditions. Modifications, required primarily at the base of the specimen, included replacing the column base plates, and adding column flange cover plates, column web doubler plates, beam-column transverse stiffeners, and a base perimeter beam (collector beam). Specimen details and boundary conditions were designed as described below.

3.2.1 *Base connection*

The connection at the base of the pier legs must be detailed to resist translation (sliding) in the two horizontal directions, to allow vertical translation (uplift) from the support during rocking, and to accommodate load cells placed beneath the base of each pier leg to record pier base reactions during testing. Connection of the pier base to the load cells was done through a horizontal bearing "pit" connection using angle members bolted to the top of each load cell as shown in Figure 3. No resistance was provided vertically through this connection except for a negligible amount of friction that may occur along an angle's leg

Figure 2. Rocking truss pier specimen on 6DOF shake table.

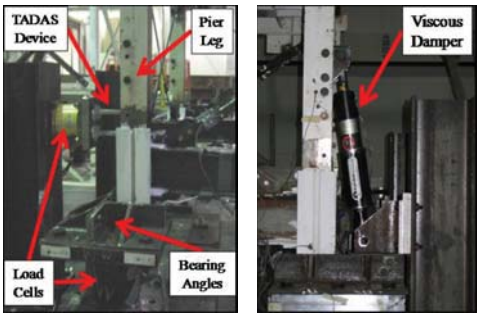

(a) (b)

Figure 3. Base connection.

as the pier leg uplifts from the load cell. The angles were only placed on the two outer sides of the load cells in contact with the two outer sides of the column base plates such that the horizontal shear force of the pier would not be transferred at the base of the uplifting pier legs. The base connection is also capable of transferring torsion in the pier that may develop as a result of accidental eccentricities.

3.2.2 *Pier diagonals*

Pier diagonals were designed to meet similitude and strength requirements. The cross-sectional area of the diagonal members (A_{dmi}) were sized such that the fixed-base and vertical periods of the specimen were close to that required by similitude and would have the required tension strength to resist demands during the rocking response. High-strength circular threaded rod (ASTM A193 B7, σ_y = 869 MPa) diagonal bracing members with a 9.5 mm diameter were used. Since buckling strength didn't scale proportionally, and these members, with effectively no buckling strength, would have undergone elastic buckling during testing, creating a tension-only bracing system, all diagonal bracing members were pre-tensioned to a prescribed axial force level such that these members would remain in tension throughout testing. The pre-tensioning was achieved by using right and left-handed threaded rod for the bracing members and connecting them with a reverse threaded hex coupler.

3.2.3 *Mass connection*

Connection of a bridge deck to its piers is typically achieved through the use of some form of bearing (rocker, pot, elastomeric, cylindrical, spherical; AASHTO, 1998). Each type of bearing transfers gravity loads and seismic inertia forces between the deck and pier by different mechanisms. For the specimen, the steel plates were connected to the steel pier using 16–9.5 mm diameter, fully tensioned high-strength threaded rods (ASTM A193 B7) through the 2–90 mm thick steel mass plates, a double concave hardened steel bearing, mild-steel connection plate, and 2–19.1 mm plate washers. The shear force was transferred through friction between each piece.

3.3 *Passive energy dissipation devices*

Passive energy dissipation (or passive control) devices were installed between the pier foundation (i.e. the shake table in this case) and the base of each pier leg. Two types of devices were used in this experimental study, namely: steel yielding devices and viscous dampers.

3.3.1 *Steel yielding devices*

TADAS devices (Tsai et. al. 1993) were used during the testing which consist of cantilever triangular plates bent about their minor axis that yield in flexure uniformly along their length when a shear force is applied at their free end. Three sets of devices were designed and fabricated with local strength ratios (η_L) of 1.0, 0.67, and 0.33 to observe the influence on response. The local strength ratio is an important parameter in design of the controlled rocking pier using steel yielding devices and is defined for 4-legged piers as:

$$\eta_L = \frac{4 \cdot F_d}{w_v} \tag{1}$$

where $F_d = V_{pT}$ = plastic capacity of the device and w_v = vertical weight tributary to the pier. A photograph of the connection of the TADAS device to the specimen is shown in Figure 3.

3.3.2 *Viscous dampers*

The controlled rocking response with viscous dampers was also investigated using a single set of nonlinear viscous dampers. The viscous dampers were implemented in a very similar manner to the TADAS devices, as seen in Figure 3. The key design parameters using such devices are the peak output force and maximum stroke of the damper. Nonlinear dampers of this type have a force output, dependent on the velocity across the damper equal to:

$$F_{vdo} = c_m \cdot \mathrm{sgn}(v) \cdot |v|^{\alpha} \, dm \tag{2}$$

where c_m = damping coefficient of 1.32 kN (sec/mm)$^{\alpha}$, v = relative velocity across the two ends of the damper, sgn = sign function, and α_{dm} = damping exponent of 0.50. The selected dampers had a stroke of ±31.75 mm, although when implemented in the controlled rocking system considered here, they only extended in a single direction as the pier legs uplifted from their base.

4 LOADING SYSTEM, INSTRUMENTATION, AND DATA ACQUISITION

The shake table used for this project can achieve a nominal acceleration performance of 1.15 g in each of its horizontal and vertical directions with a 20-ton rigid specimen, with maximum displacements of ±5.9 and ±2.9 inches in the horizontal and vertical directions, respectively.

Instrumentation used included accelerometers, string potentiometers, 8 strain gauge based load cells, and strain gauges. The entire specimen was supported on 4 large-capacity load cells that measured the base reactions. During testing with the viscous dampers, additional load cells were attached in-line with the damper shaft to measure damper force. A Krypton K600 high performance dynamic mobile coordinate measurement machine was used to measure displacements near the base of the structure. All instrumentation signals were low-pass filtered at a cut-off frequency of 50 Hz and sampled at a rate of 128 Hz.

5 BASE EXCITATION

The input excitation to the shake table included banded white noise excitation for dynamic characterization of the specimen, and seismic ground motion histories for evaluation of response. The seismic ground motions included the Newhall record from the 1994 Northridge earthquake and a synthetically generated record. All three acceleration components (2 horizontal and vertical) from each record were simultaneously applied to each specimen. Per similitude scaling laws, acceleration amplitude was unscaled and the time of the record was scaled by a factor of 2.24. The target pseudo-acceleration response spectrum of each component of motion for each record, at model scale, is shown in Figure 4.

6 TESTING PROGRAM

Each set-up (η_L = 0, 0.33, 0.67, 1.0, and η_{Lv}) was subjected to a white noise test, the Newhall record at 100% amplitude, and followed by the Synthetic record also at 100%. After that, different excitation records were run at higher amplitude (150% or more) for different set-ups. All tests were followed by a white noise test to observe any changes in the dynamic properties of the specimen.

7 RESULTS

Test results presented below include identification of the specimen's dynamic characteristics from white noise excitations, and results from seismic excitation with motion amplitudes of 100% of the target motion or greater. The peak response of each test is compared with design predictions and advanced analysis methods.

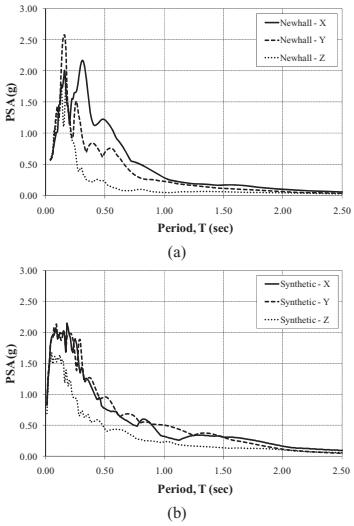

Figure 4. Target pseudo-acceleration spectra in model scale (a) Newhall record and (b) synthetic motion.

7.1 *Dynamic characteristics*

Response of the model structure during white noise excitation was limited to the elastic range of response, thus providing the fixed base pier properties; it could not capture system behavior after uplift. The mode shapes, frequencies, and damping ratios of the structure were determined using a modal identification technique based on pier transfer function response (Bendat and Piersol, 1980).

Initial white noise tests showed that the specimen had a "fixed-base" frequency of approximately 2.5 Hz (T_{om} = 0.40 sec). The specimen's inherent equivalent viscous damping, calculated both by the frequency response analysis using the half-power (bandwidth) method and by the logarithmic decrement method (Clough and Penzien, 1975), was determined to be approximately 2.5% of critical.

7.2 *Example response history results*

An example set of response history results is shown in Figure 5 for the Synthetic record input scaled to 150% of the target motion. Response of the pier with no control devices attached (η_L = 0, free rocking), steel yielding devices with η_L = 1.0 attached, and viscous dampers attached (η_{Lv}) at the base are shown in the figure. The pier relative displacements in the X-direction and device hysteretic behavior (for a single device) are presented here. The relative pier displacement is shown to return to zero following the

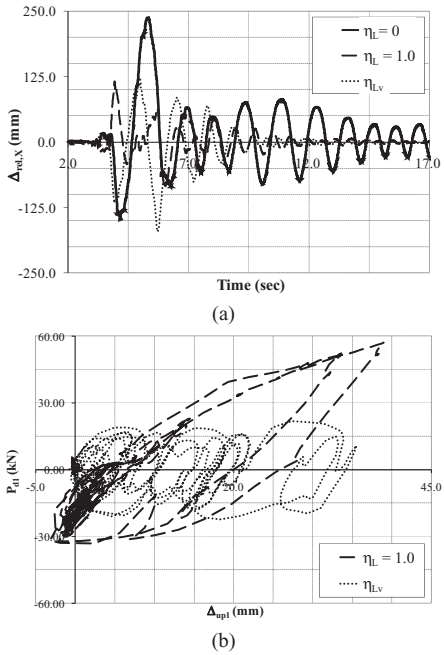

Figure 5. Sample experimental response results for synthetic motion scaled to 150%, comparison of free rocking (η_L= 0), steel yielding devices (η_L = 1.0), and viscous dampers (η_{Lv}) (a) relative pier x-displacement and (b) device hysteretic behavior.

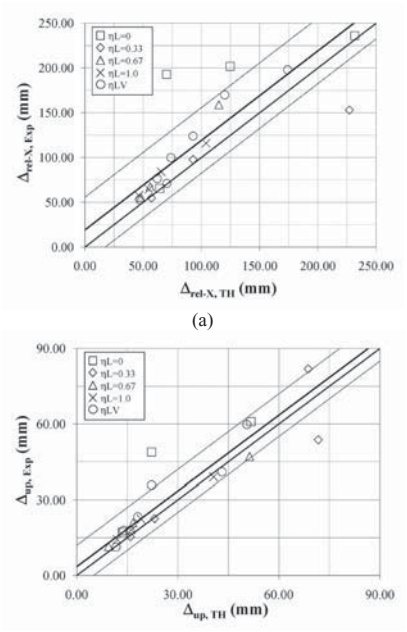

Figure 6. Experimental results comparison with time history analysis: (a) pier relative displacement in X-direction, (b) pier leg uplifting displacement.

input excitation due to the self-centering ability of the system.

7.3 *Comparison of experimental results with nonlinear time history analysis*

The response of the experimental specimen was predicted analytically using nonlinear time history analysis. Comparison is made between the peak experimental response quantities and peak response results from time history analysis.

The experimental and time history analytical results are compared in terms of peak relative displacement (X- and Y-direction) and peak uplift displacement in Figure 6 where subscripts "Exp" refers to the experimental results and "TH" refers to the results from time history analysis. Separate data points are shown on the figures for each set-up considered. A solid, dark line is plotted for $Q_{Exp} = Q_{Analytical}$ (Q referring in general to a peak response quantity). This line defines a boundary for each data point that represents conservative (below line) and unconservative (above line) prediction of response. The second solid line represents the average difference of the data from this boundary.Two dotted lines are also shown on the plots, corresponding to the mean difference of the data plus and minus one standard deviation of the data. Figure 6a and 6b show a good correlation between the experimental and time history analysis results in terms of maximum relative and uplifting displacement.

7.4 *Comparison of experimental results with design predictions*

The relative pier displacement ($\Delta_{rel,Design}$) is predicted using a simplified method of analysis that has been presented in Pollino and Bruneau (2008b) and is based on the capacity spectrum analysis method. The design uplifting displacement ($\Delta_{up,Design}$) is predicted using design equations derived from fundamental research. Comparison of the experimental and the simplified methods of analysis are shown in Figure 7 and are made in an identical manner as was done for the time history results.

The figure shows that the simplified analysis method yields displacement results that compare closely to the experimental results until the predicted relative pier displacements exceeded approximately 100 mm where the experimental results were larger than predicted by 150% to 200%. With exception of two data points, all of these outlier points for the relative displacement are for $\eta_L = 0$ or the viscous damper tests. Taking a closer look at the use of the capacity spectrum method for these cases, it was found that for those systems, having large secant periods, low

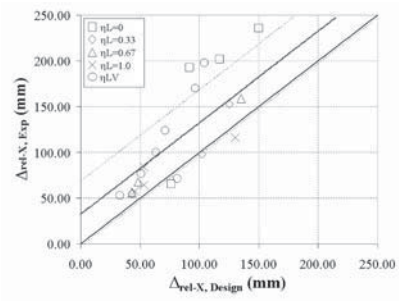

(a)

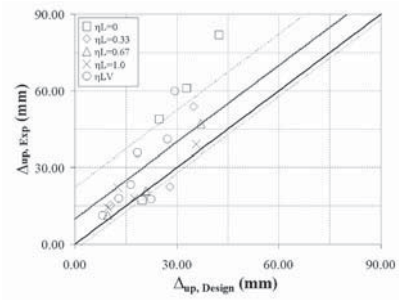

(b)

Figure 7. Experimental results comparison with design predictions: (a) pier relative displacement in X-direction, (b) pier leg uplifting displacement.

yield strength, and very low or negative post-yield stiffness (due to P-Δ effect), the intersection of the spectral capacity and demand curves occurs in a range of the spectrum that does not match the target spectrum well.

8 SUMMARY AND CONCLUSIONS

An experimental program was performed for a one-fifth length scale, 4-legged bridge pier specimen. The passive control devices used during the testing included both steel yielding devices (TADAS) and fluid viscous dampers. The specimen was subjected to three components of seismic ground motion (X+Y+Z) using both recorded and synthetically generated motions. White noise testing revealed that the "fixed-base" horizontal period in each direction was equal to 0.40 sec and that the structure had an inherent damping of approximately 2.5% of critical. Many seismic tests were performed that generated a maximum relative pier displacement of 236 mm (3.9% drift) and 82 mm of uplift. The specimen was not damaged during the testing program and re-centered following each test.

The results of the testing program were used to observe overall dynamic behavior and for verification of past research fundamental controlled rocking behavior and analytical modeling. There were a few instances in the prediction of the maximum displacement of the experimental specimen in which the simplified analysis approach provided displacements 30%–50% below that observed in experiments. Also, the maximum uplifting displacements may be influenced by the vertical ground displacements which are not accounted for in the prediction of displacements.

Simplified methods of analysis for multi-component excitation were found to provide reasonable prediction of response for most cases.

ACKNOWLEDGEMENTS

This research was supported in part by the Federal Highway Administration under contract number DTFH61-98-C-00094 to the Multidisciplinary Center for Earthquake Engineering Research. However, any opinions, findings, conclusions, and recommendations presented in this paper are those of the authors and do not necessarily reflect the views of the sponsors.

REFERENCES

AASHTO (1998). *LRFD Bridge Design Specifications*, American Association of State Highway and Transportation Officials, Washington, D.C.

Bendat and Piersol (1980). *Engineering Applications of Correlation and Spectral Analysis*, John Wiley and Sons, New York, NY.

Clough and Penzien (1975). *Dynamics of Structures*, McGraw-Hill, Inc., New York.

Dowdell and Hamersley (2001). "Lions' Gate Bridge North Approach: Seismic Retrofit", Behaviour Steel Structures in Seismic Areas: Proceedings of the Third International Conference: STESSA 2000; Montreal, Canada, August 21–24, 2000, pp. 319–326.

Harris and Sabnis (1999). *Structural Modeling and Experimental Techniques* (2nd Edition), CRC Press LLC, Boca Raton, FL.

Pollino and Bruneau (2007). "Seismic Retrofit of Bridge Steel Truss Piers Using a Controlled Rocking Approach", ASCE Journal of Bridge Engineering, Vol.12, No.5, pp. 600–610.

Pollino and Bruneau (2008a). "Dynamic Seismic Response of Controlled Rocking Bridge Steel Truss Piers", Engineering Structures Journal, Vol.30, No.6, p. 1667–1676.

Pollino and Bruneau (2008b). "Analytical and Experimental Investigation of a Controlled Rocking Approach for Seismic Protection of Bridge Steel Truss Piers", *Technical Report MCEER -08-0003*, Multidisciplinary Center for Earthquake Engineering Research, State University of New York at Buffalo, Buffalo, NY.

Tsai, K.C., Chen, H.W., Hong, C.P., and Su, Y.F. (1993). "Design of Steel Triangular Plate Energy Absorbers for Seismic-Resistant Construction", Earthquake Spectra, EERI, Vol. 9, No. 3, pp. 505–528.